ORIGINAL RESEARCH

Atrioventricular Node Slow-Pathway Ablation Reduces Atrial Fibrillation Inducibility: A Neuronal Mechanism

Xiaomeng Yin, MD, PhD;* Yutao Xi, MD, PhD;* Shulong Zhang, MD, PhD; Yunlong Xia, MD, PhD; Lianjun Gao, MD, PhD; Jinqiu Liu, MD, PhD; Nancy Cheng, MD; Qi Chen, MD, PhD; Jie Cheng, MD, PhD; Yanzong Yang, MD, PhD

***Background*—**Radiofrequency ablation (RFA) for atrioventricular nodal reentrant tachycardia appears to reduce atrial tachycardia, which might relate to parasympathetic denervation at cardiac ganglionated plexuses.

***Methods and Results*—**Compared to 7 control canines without RFA, in 14 canines, RFA at the bottom of Koch's triangle attenuated vagal stimulation–induced effective refractory periods prolongation in atrioventricular nodal and discontinuous atrioventricular conduction curves but had no effect on the sinoatrial node. RFA attenuated vagal stimulation–induced atrial effective refractory periods shortening and vulnerability window of atrial fibrillation widening in the inferior right atrium and proximal coronary sinus but not in the high right atrium and distal coronary sinus. Moreover, RFA anatomically impaired the epicardial ganglionated plexuses at the inferior vena cava inferior left atrial junction. This method was also investigated in 42 patients who had undergone ablation of atrioventricular nodal reentrant tachycardia, or 12 with an accessory pathway (AP) at the posterior septum (AP-PS), and 34 patients who had an AP at the free wall as control. In patients with atrioventricular nodal reentrant tachycardia and AP-PS, RFA at the bottom of Koch's triangle prolonged atrial effective refractory periods and reduced vulnerability windows of atrial fibrillation widening at the inferior right atrium, distal coronary sinus and proximal coronary sinus but not the high right atrium. In patients with AP-free wall, RFA had no significant atrial effects.

***Conclusions*—**RFA at the bottom of Koch's triangle attenuated local autonomic innervation in the atrioventricular node and atria, decreased vagal stimulation–induced discontinuous atrioventricular nodal conduction, and reduced atrial fibrillation inducibility due to impaired ganglionated plexuses. In patients with atrioventricular nodal reentrant tachycardia or AP-PS, RFA prolonged atrial effective refractory periods, and narrowed vulnerability windows of atrial fibrillation. **(*J Am Heart Assoc*. 2016;5:e003083 doi: 10.1161/JAHA.115.003083)**

Key Words: atrial fibrillation • atrioventricular node • ganglion plexus • slow-pathway • vagal stimulation

In patients with atrioventricular nodal reentrant tachycardia (AVNRT), the effects of radiofrequency ablation (RFA) on the sinus node, atrioventricular node (AVN), and atrial electrophysiologic properties are unclear. Previous studies had suggested the contribution of neuronal denervation caused by RFA.[1–7] However, experimental evidence of parasympathetic denervation is lacking.

In the vagal pathways, the fat pad at the junction of the inferior vena cava and inferior left atrium contains the right inferior ganglionated plexus ($GP_{IVC\text{-}ICA}$), from which convergence points of vagal stimulation (VS) project into the AVN region.[8–10] Researchers have suggested that the $GP_{IVC\text{-}ICA}$ might be the "gateway" or integration center for extrinsic innervation to the AVN.[8,11] Anatomically, the $GP_{IVC\text{-}ICA}$ lies adjacent to the endocardially located coronary sinus ostium.[12] Studies have shown that ablation in this area inhibits vagal activity in the AVN, as well as in the atria.[3,4,13] Moreover, ablation of the "slow pathway" in patients with AVNRT decreases vulnerability to pacing-induced atrial fibrillation (AF),[3,14] suggesting that local parasympathetic denervation is a possible mechanism. Therefore, we hypothesized that ablation at the bottom of Koch's triangle targeting the slow pathway may result in vagal denervation due to $GP_{IVC\text{-}ICA}$ neuronal damage. We performed a canine study to determine whether such ablation alters vagal innervation in the atria and

From the First Affiliated Hospital of Dalian Medical University, Dalian, Liaoning, China (X.Y., S.Z., Y. Xia, L.G., J.L. Y.Y.); Texas Heart Institute, Houston, TX (Y. Xi); CHI St. Luke's Health – Baylor St. Luke's Medical Center, Houston, TX (N.C., Q.C., J.C.); University of Texas Medical Branch, Galveston, TX (N.C.).

*Dr Yin and Dr Xi contributed equally to this work.

Correspondence to: Yanzong Yang, MD, PhD, or Yunlong Xia, MD, PhD, The First Affiliated Hospital of Dalian Medical University, 222 Zhongshan Rd, Dalian, Liaoning, China 116011. E-mails: yyzheart@126.com, YunlongXia2014@163.com

Received December 9, 2015; accepted May 5, 2016.

atrioventricular conduction due to impaired neurons within the $GP_{IVC-ICA}$. Furthermore, we investigated whether such denervation in canines is relevant to RFA targeting the slow pathway of Koch's triangle in patients with supraventricular tachycardia (SVT).

Methods

Part I: Canine Study

Animal model preparations

The Institutional Animal Care and Use Committee of Dalian Medical University approved the experimental protocol in advance. Twenty-one mongrel dogs (10 15 kg each) in 2 groups of ablation (14 dogs) and control (7 dogs) were anesthetized with sodium pentobarbital (150 mg/kg intravenously). The dogs were ventilated with a constant volume-cycled respirator through a cuffed endotracheal tube, and blood oxygen saturation was maintained above 95%. The temperature and illumination of the operating room were kept stable throughout the experiment. Six-lead ECGs and intracardiac electrograms were recorded (Prucka 7000; GE Healthcare, Milwaukee, WI). The cut-off frequencies were 30–300 Hz for the bipolar intracardiac electrograms at a sampling frequency of 1 kHz.

Vagal stimulation

Propranolol was administered, initially as a 2-mg/kg bolus and subsequently in a maintenance dosage of 2 mg/kg per hour to inhibit sympathetic activity. Both cervical vagal trunks were exposed, and the cranial ends of the vagal nerves were ligated. Two pairs of electrodes were embedded in the caudal end of the vagosympathetic nerve track for stimulation. A rectangular pulse was delivered through a constant voltage stimulator at 20 Hz with a pulse width of 2 ms by a programmable stimulator (RST-2, Huanan Medical, Hunan, China). The VS threshold was defined as the voltage level that could decrease the heart rate (HR) by 30% or result in 2:1 atrioventricular block. Half of the threshold voltage was used to test the effect of VS on the AVN effective refractory period (ERP). The threshold voltage×2 was used to test the atrial ERP (AERP).

Catheter positioning

A decapolar catheter was used to record the signals in the proximal (CSp) and distal (CSd) portions of the coronary sinus. A deflectable duodecapolar Halo catheter was positioned in the right atrium to monitor the high right atrium (HRA) and inferior (IRA) right atrium, and a quadripolar catheter was placed in the His-bundle region. In addition, a 4-mm nonirrigated tip ablation catheter was deployed at the bottom of Koch's triangle for mapping and ablation. A quadrapolar catheter was advanced into right ventricular apex for temporary pacing. All catheters were manufactured by Cordis, Biosense Webster, Inc. (Diamond Bar, CA) and were positioned with fluoroscopic guidance (Innova 2000; GE Healthcare) (Figure 1A).

Electrophysiologic studies

An atrial pacing protocol involving a single extrastimulus was performed with a programmable multichannel stimulator (Model DF-5A; Dongfang Electric Co., Chengdu, China). The pacing amplitude was set at twice the diastolic threshold. The atrial ERP was defined as the longest coupling interval of the extrastimulus that failed to capture the local atria. The AVN ERP was defined as the longest atrial coupling interval (A1–A2) observed on the His-bundle electrograms when A did not conduct to the His bundle. To determine the atrial ERP, we performed an extrastimulus with coupling intervals of 200 ms that were progressively shortened by 10 ms with a basic drive cycle length of 250 ms at all sites. AF was defined as more than 2 s of atrial activity appearing as an irregular cycle length on the intracardiac ECG and fibrillatory waves on the surface ECG.[15] The vulnerability window (VW) for development of AF was defined as any coupling interval range of the extrastimulus at which fibrillation was induced.[16,17] The control group underwent only the baseline electrophysiology study.

Radiofrequency ablation at the bottom of Koch's triangle in canines

Radiofrequency energy was delivered at the bottom of Koch's triangle with a 4-mm nonirrigated–tip ablation catheter (Cordis; Biosense Webster Inc.) connected to Stockert (Biosense Webster Inc.). Ablation was performed by moving the tip in a point-by-point manner from the coronary sinus ostium toward the His bundle until the His signal was detected.[3] The tip was then moved back 2 mm for ablation (Figure 1B). For each ablation, energy was applied and then was stopped automatically when the abrupt impedance rose to 30 Ω above the baseline level. The highest energy given was 60 W, with a temperature threshold of 55°C and a duration of 60 s.

High-frequency stimulation

In dogs that underwent ablation at the Bottom of Koch's Triangle, the function of the $GP_{IVC-ICA}$ within Koch's triangle was assessed by delivering high-frequency stimulation (20 Hz, 10–150 V, 1–10-ms pulse width; S-88 stimulator; Grass Instruments Division, AstroNova, Inc., West Warwick, RI) to each site for 5 s. The immediate response was defined as a >50% increase in R-R intervals and a >30% increase in

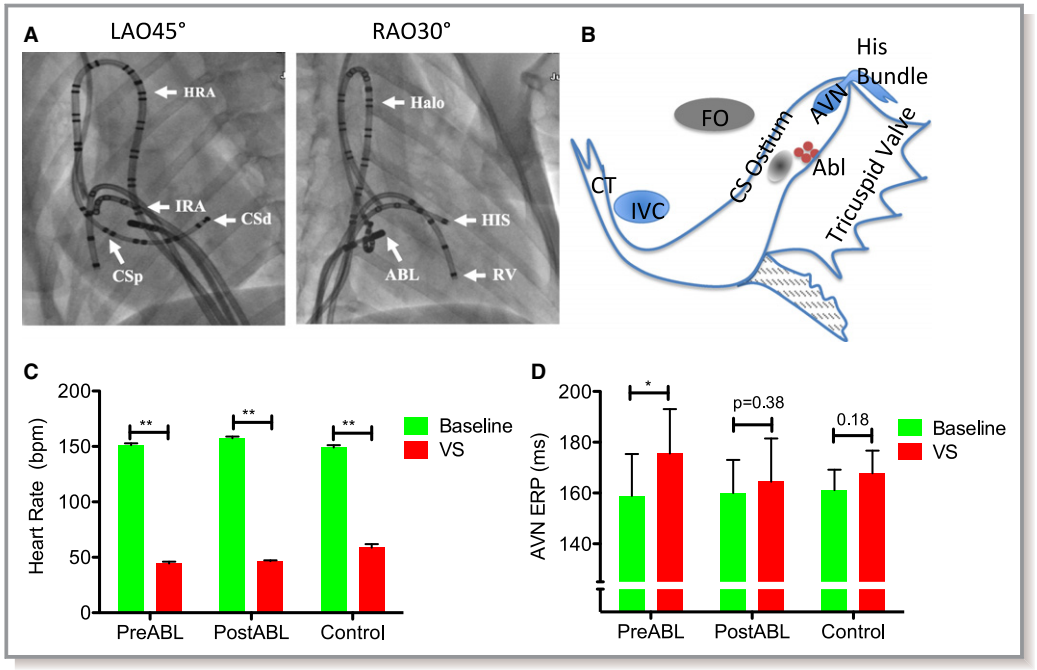

Figure 1. Effects of radiofrequency ablation (RFA) at the bottom of Koch's triangle on the heart rate (HR) and effective refractory periods (ERPs) of the atrioventricular node (AVN) in dogs. A, Catheter position; (B) Koch's triangle and RFA sites; (C) HR; (D) AVN ERPs. ABL indicates RFA sites; CSd, distal coronary sinus; CSp, proximal coronary sinus; CT, crista terminalis; FO, fossa ovalis; Halo, Halo catheter; HIS, His bundles; HRA, high right atrium; IRA, inferior right atrium; IVC, inferior vena cava; LAO, left anterior oblique; RAO, right anterior oblique; RV, right ventricle; VS, vagal stimulation. (*P<0.05; **P<0.01).

hypotension (compared to that observed without high-frequency stimulation) during stimulation.[18]

Histopathologic results

After the in vivo experiments were completed, all animals were humanely euthanized, and their hearts were removed for histologic examination. Tissue samples from Koch's triangle were excised according to the anatomic and ablation markers, fixed with 4% paraformaldehyde, embedded in paraffin wax, and cut into 10-μm- thick cross-sections. Slides were stained for microscopic examination with hematoxylin and eosin, anticholine acetyltransferase (Abcam, Cambridge, MA), and antityrosine hydroxylase (EMD Millipore, Darmstadt, Germany). The number of visible nuclei was factored for the square area of the GP visible in each field with ImageJ software (National Institutes of Health, Bethesda, MD).

Part II: Clinical Study

Ablation in patients with SVT

Between 2011 and 2013, 590 patients underwent ablation of AVNRT, an accessory pathway (AP) at the posterior septum (AP-PS), or an AP at the free wall (AP-FW) at the First Affiliate Hospital of Dalian Medical University. A total of 88 patients qualified for the current study, including 42 patients with AVNRT, 12 AP-PS, and 34 AP-FW. The patients with AP-FW served as a control group, because the ablations for AP-FW were not within the Koch's triangle. Exclusion criteria included AF; use of amiodarone; left ventricular ejection fraction <50%; congenital, ischemic, or valvular heart disease; stroke; diabetes mellitus; overweight status (body mass index >30); and renal impairment.

The study protocol was preapproved by the university's Research Development and Human Ethics Committee. Before enrolling in the study, all patients gave written informed consent. All antiarrhythmic medications were suspended for at least 5 half-lives before the procedure. In all cases, lidocaine was administered for local anesthesia at the catheter access site.

Induction of AF

The inducibility of AF was determined as in the canine study described above. The VW of AF was determined before and after ablation. Briefly, AF inducibility was evaluated by performing a programmed single extrastimulus at twice the threshold value, followed by burst atrial pacing for 5 s at twice the threshold value. Induction was repeated at least 3 times at each site. AF was defined as >2 s of atrial activity, as revealed by an irregular cycle length on the intracardiac ECG and fibrillatory waves on the surface ECG.

Statistical Analysis

Data were reported as the mean value±SD. A repeated measurement of ANOVA and ANCOVA model followed by a postestimation was used to compare 3 groups of baseline, 4 sites, and pre- and postablation on AERP and VW. Paired *t* tests were conducted between preablation and postablation values. A first-order exponential model was used to fit the curves of A-H intervals versus the A-A pacing intervals from individual dogs. A *P* value of ≤0.05 was considered significant. All tests were performed with SPSS software, Version 16.0 (IBM SPSS Statistics, Chicago, IL).

Results

Part I: Animal Study

RFA at the bottom of Koch's triangle attenuated VS-induced prolongation of AVN ERPs

Figure 1A and 1B show the location of the catheters and ablation sites, and Table 1 presents the parameters used for ablation and VS. There was no significant difference between the ablation and control groups in regard to the VS threshold. The ERPs of the sinoatrial and atrioventricular nodes, as well as of 4 atrial sites, were tested with and without VS, preablation and postablation. The HRs and the ERPs of the AVN with VS were compared pre- and postablation at the bottom of Koch's triangle. As shown in Figure 1C, RFA had no significant effect on VS-induced reduction of the HR (107±6.1 bpm preablation versus 111±6.2 bpm postablation; *P*=0.21). The differences in HR responses to VS were significant preablation (152±6 versus 46±6 bpm; *P*<0.01) and postablation (158±5 versus 47±3 bpm; *P*<0.01), but VS-induced reductions in HR were comparable pre- and postablation (106.7±6.0 versus 110.9±6.2 bpm; *P*=0.08).

Table 1. Canine Study: Parameters for Ablation and VS

Parameters	Ablation (n=14)	Control (n=7)
Ablation wattage, W	30.5±2.15	—
Ablation time, s	169.3±10.69	—
Ablation lesions (points)	5.2±0.5	—
Ablation temperature, °C	53.5±2.07	—
VS voltage, V	7.8±0.35	7.8±0.5
VS voltage at AVN ERP testing, V*	1.3±0.07	1.3±0.09
Procedure duration, hr	4.8±0.25	1.9±0.34
Animal weight, kg	12.7±0.42	13.2±0.63

AVN ERP indicates atrioventricular nodal effective refractory periods; VS, vagal stimulation.
*11 dogs were tested for AVN ERP, because 3 dogs showed AV block with VS.

Vagal stimulation significantly prolonged the AVN ERP preablation (from 159±16 to 176±17 ms; *P*<0.05), but it produced no significant effects postablation (from 160±13 to 164±17 ms; *P*=0.38) when tested at atrial pacing cycle lengths (A-A) of 250 ms with a half threshold voltage of VS. Therefore, RFA attenuated VS-induced prolongation of the AVN ERP (postablation: 4.44±4.74 ms versus preablation: 16.67±5.53 ms; *P*<0.05) (Figure 1D). The AVN ERPs without VS were comparable to each other (*P*=0.85).

RFA at the bottom of Koch's triangle attenuated VS-induced shifts of A-H conduction–time curves

The AVN conduction time, tested as the A-H interval, was prolonged when atrial pacing cycle lengths A-A (or drive cycle lengths) were shortened from 300 to 150 ms in decrements of 10 ms in the IRA. To determine the effects of VS on the AVN conduction time, A-H conduction-time curves were compared to the A-A pacing interval pre- and postablation. As shown in Figure 2A, obtained from a representative dog, VS shifted the A-H curves toward the right, where the shift could be blocked by RFA.

During VS, the AVN conduction curves were discontinuous, or exhibited "jumping phenomena," manifested as a sudden increase in A-H and a decrement in A-A coupling intervals. The discontinuities were defined as the maximal prolongation of A-H intervals ($\Delta A–H_{max}$) during reduction of the A-A interval in 10-ms decrements. As shown in Figure 2B, VS increased the $\Delta A–H_{max}$ significantly, from 13±2 to 33±4 ms (*P*<0.01). After RFA, however, the $\Delta A–H_{max}$ response to VS was attenuated from 14±2 to 13±2 ms (*P*=0.58).

In the first-order exponential model, the time-constants (τ) of the curves were used to assess the A-H conduction intervals. As shown in Figure 2C, the τ values with VS were decreased from 88.46±7.36 to 52.03±6.99 ms (paired *P*<0.01; n=7). Postablation, the τ values were comparable with VS (75.7±8.23 ms) and without VS (83.79±9.56 ms) (paired *P*=0.06). Moreover, the changes in τ values between baseline and VS were significantly decreased postablation (12.24±3.27 ms) (paired *P* <0.05) compared to preablation (36.43±9.01 ms) (Figure 2D).

RFA at the bottom of Koch's triangle partially attenuated VS-induced atrial ERP shortening

Before RFA, VS significantly shortened the atrial ERPs at all sites compared to the ERPs at baseline (Figure 3). Additionally, VS-induced shortening of atrial ERPs was comparable among the 4 sites (ANOVA; *P*=0.11). However, after RFA, VS-shortened atrial ERPs were diverse (ANOVA; *P*<0.01). Shortened atrial ERPs were comparable preablation and postablation at sites in the HRA (ΔERP: 72±19 versus 67±22 ms; *P*=0.45) but were decreased at sites in the CSd (ΔERP: 59±7

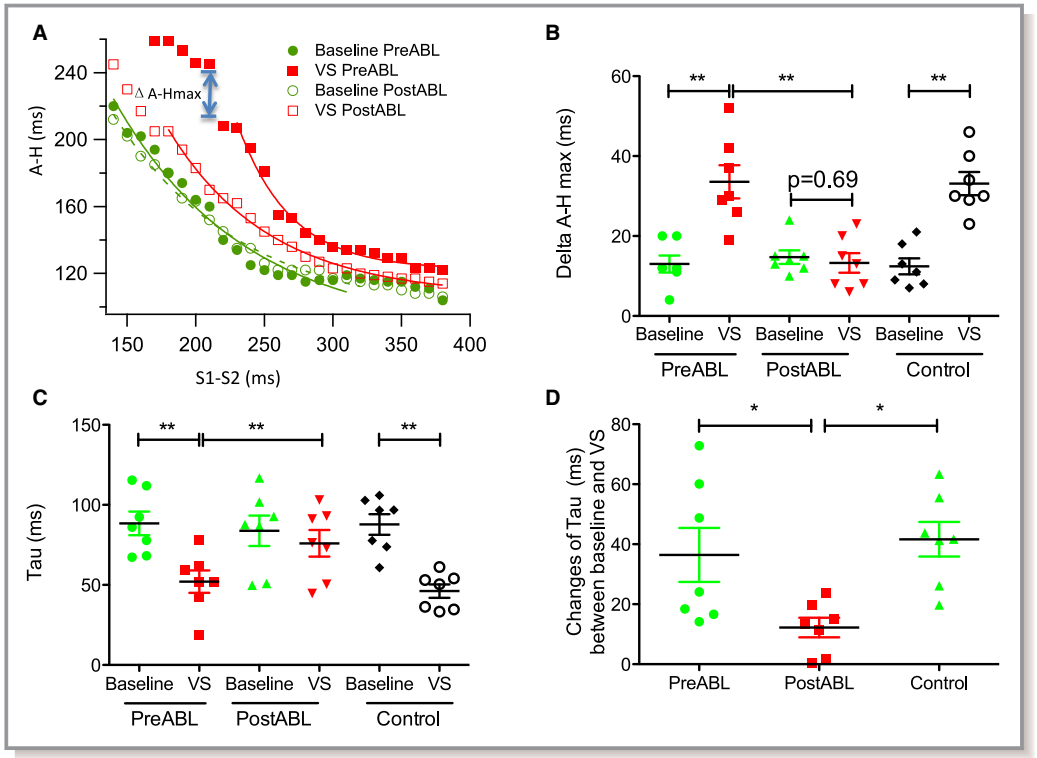

Figure 2. Effects of vagal stimulation (VS) on A-H conduction-time curves preablation (PreABL) and postablation (PostABL) at the bottom of Koch's triangle in dogs. A, Representative A–H curves from dog 3; (B) maximal vagal-induced A–H changes; (C) effects of VS on the τ value of the A–H curve fitted by first-order exponential model; (D) Changes in τ between baseline (without VS) and with VS (*P<0.05; **P<0.01).

versus 29±7 ms; P<0.05). However, VS-induced shortening of the ERP was attenuated at sites of CSp (ΔERP: 48±7 versus 6±4 ms; P<0.01) and IRA (ΔERP: 66±5 versus 11±3 ms; P<0.01).

RFA at the bottom of Koch's triangle reduced the VS-induced VWs of AF

Before and after ablation, AF was barely induced at all sites without VS, where the VWs trended to 0. Therefore, the VWs during VS were compared only for preablation versus postablation. The results showed that RFA significantly narrowed the VWs at sites in the IRA and CSp (IRA: 49±36 versus 1±3 ms; P<0.05; CSp: 45±34 versus 10±12 ms; P<0.05); however, there were no changes at sites in the HRA (63±25 versus 63±31 ms; P=0.99) and CSd (57±28 versus 35±37 ms; P=0.07) (Figure 4). At all sites, the preablation and control VWs were comparable.

Neuronal mechanism of ablation at Koch's triangle

The function of GPs was evaluated by high-frequency stimulation before and after ablation. At least 1 area of response was identified within Koch's triangle before ablation. There was no response after successful ablation. Typical response and nonresponse pressure tracings are shown in Figure 5A and 5B, respectively.

At Koch's triangle, the atrial tissues with ablation markers were collected and sliced for histologic examination. The neuronal ganglia and fibers were found on the epicardial side, located transmurally across the atrial wall from the ablation points (Figure 5). In samples from the control group, the GP was clearly seen to connect with neuronal fibers and to be surrounded by adipose tissue (Figure 5C). Both cholinergic and adrenergic neurons were detected with antibodies for choline acetyltransferase (Figure 5D) and antityrosine hydroxylase staining (Figure 5E), respectively. In addition, the neurons were severely impaired in the tissues from the RFA group (Figure 5F). The fraction of nuclear numbers in a cross-sectional area of the GPs was compared in the ablation versus control groups. In the ablation group, the fraction of the normal nuclear number in the cross-sectional area of the GPs was significantly reduced (33±8% versus 15±7%; P<0.01).

Part II: Clinical Study

Study population

Eight-eight patients (40 men and 48 women, aged 47.9±14.3 years) who had undergone RFA for SVT at our

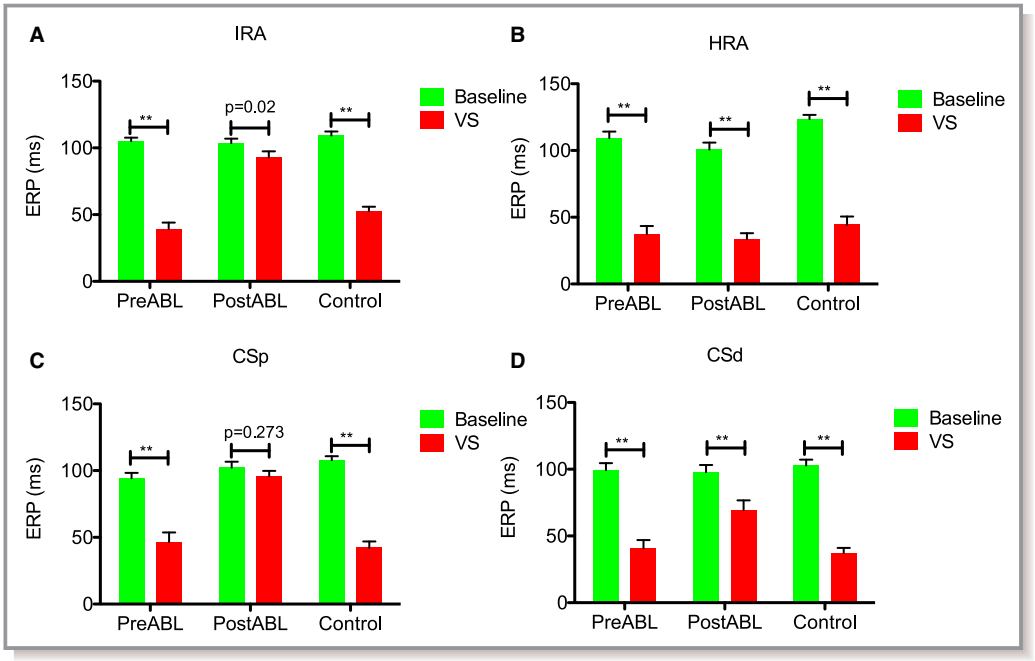

Figure 3. Vagal-stimulation (VS)–induced atrial effective refractory periods (ERPs) preablation and postablation at the bottom of Koch's triangle in dogs. A, Inferior right atrium (IRA); (B) high right atrium (HRA); (C) proximal coronary sinus (CSp); (D) distal coronary sinus (CSd). PreABL indicates preablation; PostABL, postablation (**P<0.01).

institution were enrolled in the study. The patients were divided into 3 groups, depending on the site of ablation: AVNRT (n=42), AP-FW (n=34), and AP-PS (n=12). The SVT had lasted for a mean period of 11.1±7.6 years, and was heterogeneous among 3 groups (P<0.05). The AP-FW patients have the longest duration, and AVNRT have the shortest.

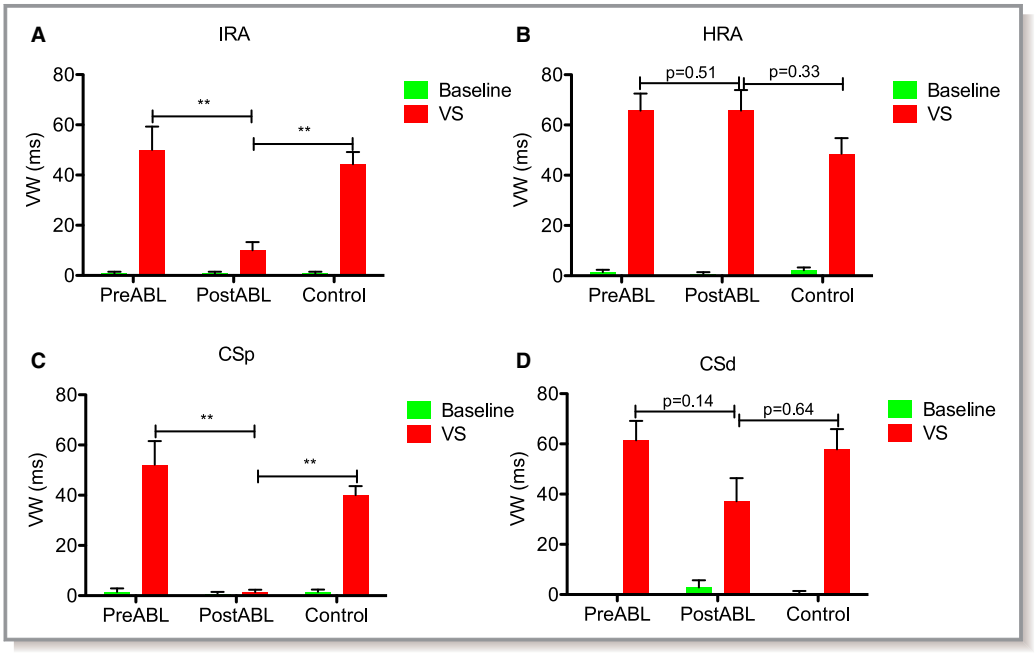

Figure 4. Vagal-stimulation (VS)–induced changes in the vulnerability windows (VWs) of atrial fibrillation preablation (PreABL) and postablation (PostABL) at the bottom of Koch's triangle in dogs. A, Inferior right atrium (IRA); (B) high right atrium (HRA); (C) proximal coronary sinus (CSp); (D) distal coronary sinus (CSd) (**P<0.01).

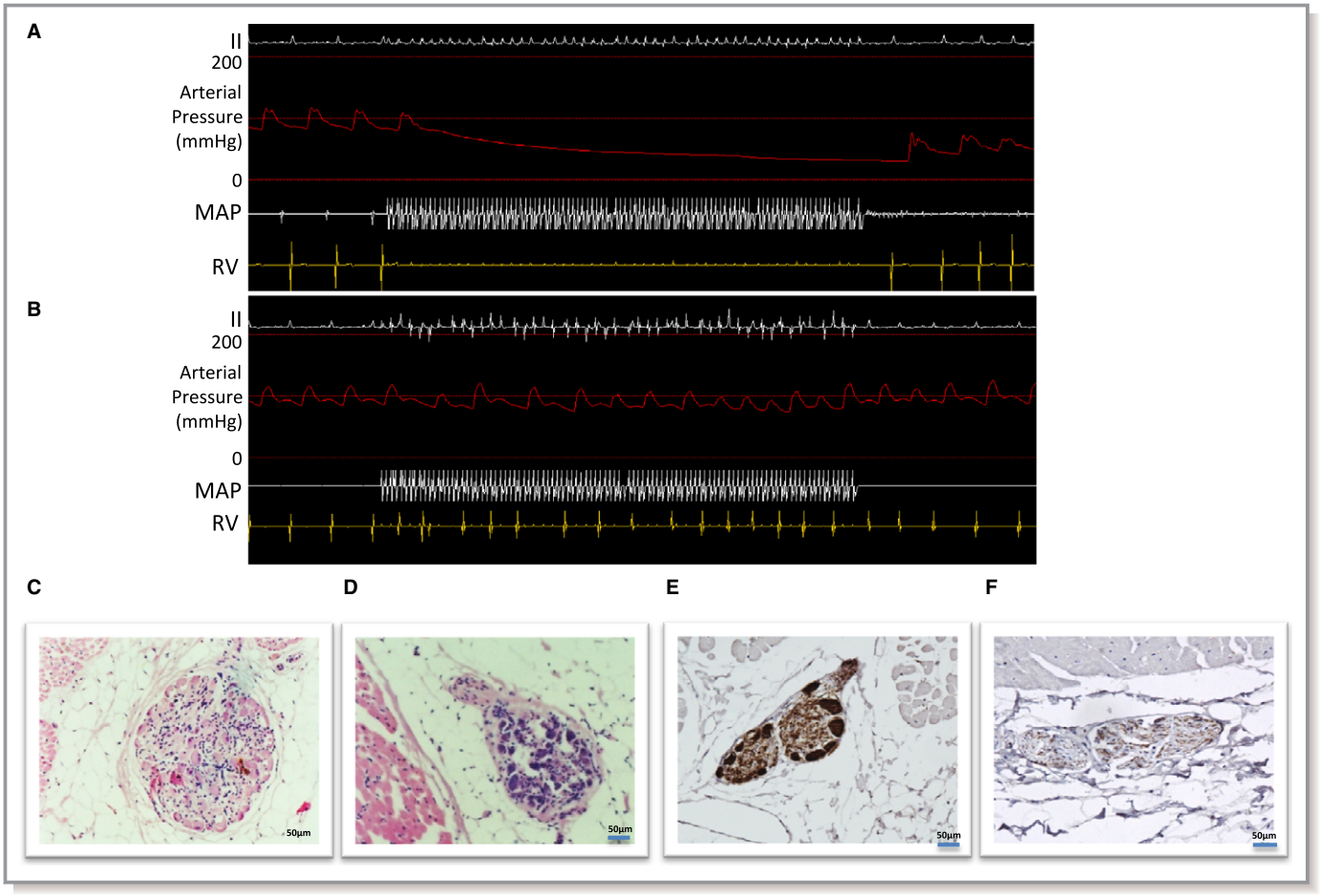

Figure 5. Distributions of neurons at the bottom of Koch's triangle in dogs. Traces of arterial pressure and ventricular rates showing responses to high-frequency stimulation in dogs: (A) positive response; (B) negative response. C through F, Histologic stains of atrial tissue from Koch's triangle in dogs (see text): (C) hematoxylin and eosin (H&E) stain preablation; (D) choline acetyltransferase stain; (E) tyrosine hydroxylase stain; (F) H&E stain postablation. Bar: 50 μm. II indicates electrocardiographic lead II; MAP, mapping and ablation catheter; RV, right ventricle.

There was no significant intergroup difference in heart chamber size or diastolic function (Table 1). Table 2 shows the group's basic characteristics.

Effects of slow-pathway ablation on the sinus node and AVN in SVT patients

In accordance with SVT procedural guidelines, accessory pathways were mapped, and the following RFA protocol was used to treat AP-PS and AP-FW. The end point of ablation was elimination of the slow pathway, as indicated by the presence of junctional rhythm and absence of induced junctional reentry. The median number of RFA applications was 3 (range, 1 8). The averaged ablation wattage and time were less for AVNRT than for AP-PS ($P<0.01$) and AP-FW ($P<0.01$) (Figure 6A and 6B). After RFA, sinus rate increased in the AVNRT group (paired $P<0.05$) and tended to increase in the AP-PS group ($P=0.08$), but the AP-FW group had no significant changes in sinus rate ($P=0.37$) (Figure 6C). The antegrade AVN ERPs were prolonged in patients with AVNRT ($P<0.05$) and AP-FW ($P<0.05$), but changes in the ERPs were similar in both groups ($P=0.69$). However, the antegrade AVN ERP showed a trend toward shortening in patients with AP-PS ($P=0.09$) (Figure 6D).

Effects of slow-pathway ablation on atrial ERPs and VWs of AF in SVT patients

Atrial ERPs at 4 sites were tested in the 3 groups, at the preablation and postablation (Figure 7A through 7D). RFA showed diverse effects among groups and sites ($P<0.01$). RFA in AVRNT and AP-PS patients significantly affected the atrial ERP at sites of CSd, CSp, and IRA ($P<0.05$). However, RFA had no significant effect on all sites in AP-FW patients. Also, RFA had no significant effects at sites of HRA for all 3 groups of patients ($P=0.88$). For effects on VW, RFA showed diverse effects among groups and sites ($P<0.01$). Similarly, RFA showed diverse effects among groups and sites ($P<0.01$). RFA significantly narrowed the VWs of AF in the AVNRT and AP-PS patients at sites of CSd, CSp, and IRA ($P<0.05$), but produced

Table 2. Basic Patient Characteristics

Characteristic	AVNRT (n=42)	AP-FW (n=33)	AP-PS (n=12)	*P* Value
Male (%)	17 (40%)	17 (52%)	6 (50%)	0.616
Age, y	50.3±13.9	45.3±14.5	47.0±15.2	0.307
Duration of tachycardia, mo	8.8±7.1	13.8±8.0*	11.1±6.1	0.016
Echocardiography				
LVEDd, mm	45.1±3.1	44.6±3.2	44.3±3.7	0.651
LVESd, mm	27.5±2.1	26.7±2.4	26.8±2.6	0.272
LA, mm	34.6±1.6	33.8±2.4	34.3±1.6	0.218
LVEF, %	62.9±4.9	64.2±4.7	64.2±3.7	0.459

AP-FW indicates atrioventricular reentrant tachycardia at the free wall; AP-PS, atrioventricular reentrant tachycardia at the posterior wall; AVNRT, atrioventricular nodal reentrant tachycardia; LA, left atrial dimension; LVEDd, left ventricular end-diastolic dimension; LVEF, left ventricular ejection fraction; LVESd, left ventricular end-systolic dimension.
**P* vs AVNRT.

no significant effects at all sites in the AP-FW patients. Moreover, there were no significant changes at sites in the HRA in any of the 3 groups (Figure 7E through 7H). Furthermore, a regression analysis indicated that the duration of SVT history has no significant contribution to the diversity of atrial and atrioventricular node ERP and VW to AF.

Discussion

Main Findings

In the present study, we demonstrated in canines that RFA at the bottom of Koch's triangle, where the $GP_{IVC\text{-}ICA}$ is located epicardially, attenuated the following VS-induced changes: (1) prolongation of the AVN ERP, (2) shifts of the AVN conduction curves, (3) shortening of the atrial ERP, and (4) widening of the VW of AF. Furthermore, in patients with AVNRT and AP-PS, ablation of the slow pathway within Koch's triangle prolonged the atrial ERPs and reduced AF inducibility. However, ablation had no significant effects on the atrial ERPs in AP-FW patients, in whom the ablation sites were not located close to Koch's triangle.

Role of VS in Dual AVN Physiology

In the mid-1950s, Moe et al[19] described dual AVN physiology of the canine heart. Not until 1973, however, did Denes et al[20] describe reentry of the AVN based on the theory of

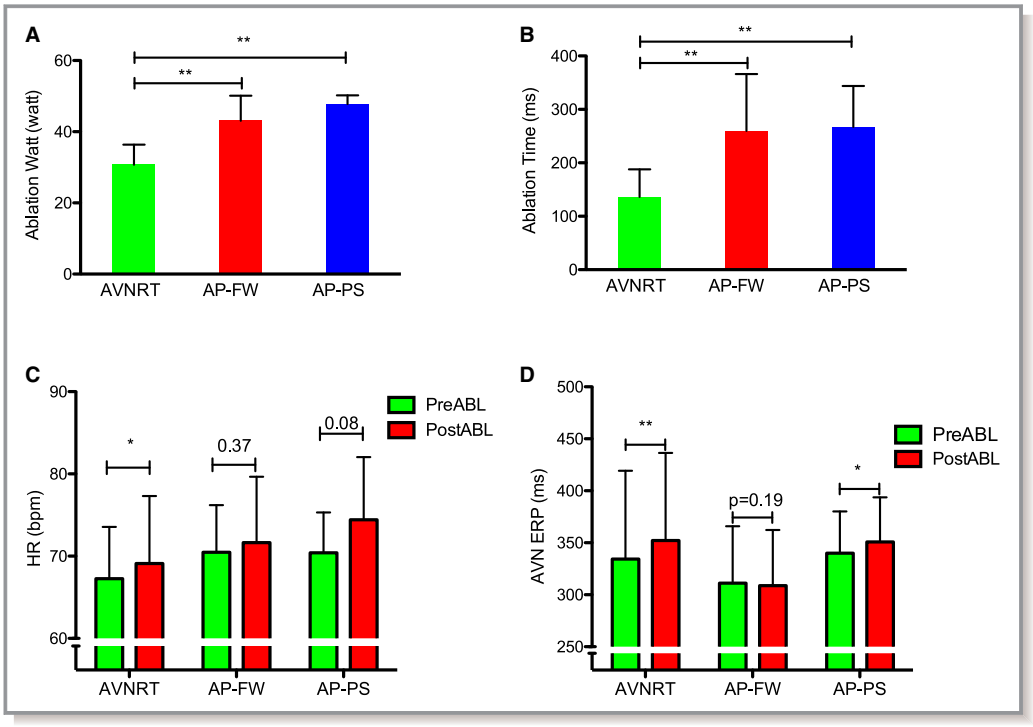

Figure 6. Effects of radiofrequency ablation of the slow pathway on the heart rate (HR) and effective refractory periods of the atrioventricular node (AVN ERPs) in patients with supraventricular tachycardia. A, Average ablation wattage; (B) average ablation times; (C) heart rate; (D) AVN ERPs. AP-FW, accessory pathways at the free wall; AP-PS, accessory pathways at the posterior wall; AVNRT, atrioventricular nodal reentrant tachycardia; PreABL, preablation; PostABL, postablation (**P*<0.05; ***P*<0.01).

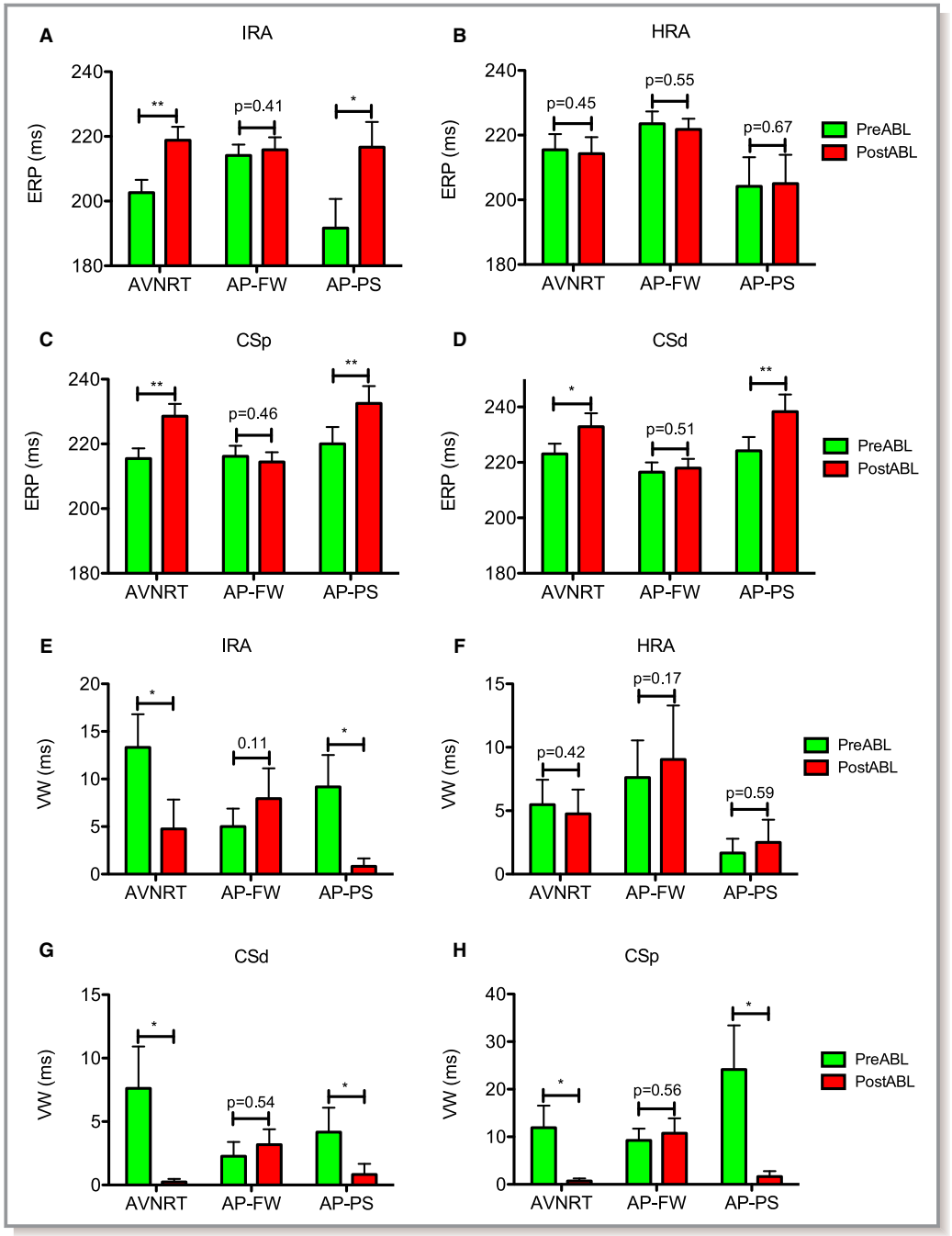

Figure 7. Effects of radiofrequency ablation of the slow pathway on atrial effective refractory periods (ERPs) and vulnerability windows (VWs) in patients with supraventricular tachycardia. A and E, inferior right atrium (IRA); (B and F) high right atrium (HRA); (C and G) proximal coronary sinus (CSp); (D and H) distal coronary sinus (CSd). AP-FW indicates accessory pathways at the free wall; AP-PS, accessory pathways at the posterior wall; AVNRT, atrioventricular nodal reentrant tachycardia; PreABL, before radiofrequency ablation at the bottom of Koch's triangle; PostABL, after radiofrequency ablation at the bottom of Koch's triangle. **P*<0.05, ***P*<0.01 vs. PreABL.

functional longitudinal dissociation of dual AVN physiology, which is the mechanism that underlies AVNRT.[21,22] Nevertheless, the precise anatomic site and nature of the pathways remain unknown. Chiou CW et al[23] reported that responses to VS were different in the slow versus fast pathways: VS significantly prolonged the ERP of antegrade conduction in the fast pathway but had no effect on retrograde or antegrade conduction in the slow pathway. In the typical slow–fast form of AVNRT, VS might be involved in formation of the AVNRT circuit in the pattern of antegrade conduction in the slow

pathway, as well as retrograde conduction in the fast pathway. Also, Mazgalev et al[24–26] used VS to induce AVNRT in isolated rabbit hearts, thus providing evidence of VS modulation in dual AVN physiology. In the present study, VS amplified the difference in conduction between the slow and fast pathways, thereby manifesting as discontinuous AVN conduction curves.

Hyperactive VS Triggers SVT

Ablation of the slow pathway has become an efficient, well-established treatment for AVNRT.[27] However, evidence of anatomic reentry or circulating pathways is lacking and the mechanism of AVNRT remains controversial. In our study, after ablation of the slow pathway, discontinuous atrioventricular conduction was detectible in certain cases, but SVT could not be induced. In contrast, some AVNRT patients exhibited a smooth AVN conduction curve.[28] This suggests that dual AVN physiology is not an exclusive mechanism of AVNRT.[28] Therefore, like others, we have demonstrated the important contributions of vagal activities in triggering SVT. Ablation at the bottom of Koch's triangle attenuated the vagal-related heterogeneity in atrioventricular conduction, thereby reducing the potential for reentry, as confirmed by impairment of the GP and blockade of vagal activity after ablation.

Ablation of the Slow Pathway May Prevent AF Induction

Little information exists about the specific distribution of the vagal pathways to the atrial myocardium. In this study, RFA was delivered to the endocardial tissues at the bottom of Koch's triangle, which mirrored the epicardial fat pad at the $GP_{IVC\text{-}LA}$.[29] Histologic results confirmed that RFA impaired the nerve fibers and neurons located in the epicardial fat pad. Ablation attenuated the ERP shortening response to VS near the region of ablation but not in any remote areas; this indicated that ablation at the bottom of Koch's triangle resulted in remarkable denervation of the atrial vagus nerves. Previous studies showed that innervation of the $GP_{IVC\text{-}LA}$ is the integration center for extrinsic vagal pathways. Autonomic branches from both the right and left vagus nerves pass through the $GP_{IVC\text{-}LA}$ to the AVN.[8,11] Ablation of the $GP_{IVC\text{-}LA}$ both attenuated VS-induced VW widening and increased AF inducibility.[30]

Clinical Implications

Ablation of the intrinsic cardiac autonomic nervous system, particularly targeting of the GP, has been shown to increase the success of AF ablation. Indeed, it has been suggested that RFA for AVNRT results in parasympathetic denervation with inadvertent tachycardia. However, it is not clear whether such denervation affects the atria. In the present study, we showed that RFA of the slow pathway at the bottom of Koch's triangle impaired the epicardial $GP_{IVC\text{-}LA}$ in canine atria and resulted in vagal denervation in the atria and AVN. In patients with AVNRT, slow-pathway ablation has been well documented as having a high success rate, but the anatomic mechanism for the reentrant or circulating pathway is unknown. In our dogs, VS induced discontinuities or similar "jumping phenomena" in AVN conduction curves, thereby indicating the role of vagal activity in AVNRT formation. This role was supported by the observation of increased vagal activity in patients with AVNRT.[23] Moreover, in the present study, slow-pathway ablation in patients with AVNRT and AP-PS altered the atrial ERP and AF inducibility.

Limitations

Lack of information concerning the incidence of—and vulnerability to—AF in these patients limited our ability to determine whether or not ablation contributed to AF. Follow-up studies of these patients are ongoing regarding the incidence of AF and other arrhythmias. Also, as a retrospective study, the present study may not be representative of the general population and may be prone to selection bias due to lacking of power analysis and sample size. However, the present study indicates that the area of Koch's triangle might need more attention. Future prospective studies are warranted to optimize the strategies for AF.

The location of the $GP_{IVC\text{-}LA}$ was not identified with high-frequency stimulation before ablation. The endocardial ablation of the $GP_{IVC\text{-}LA}$ might have been confounded with tissue ablation. Although the canine histologic findings indicated that GP structure was impaired after ablation, the location of the $GP_{IVC\text{-}LA}$ may have differed from subject to subject. Only ERPs were tested and compared in this study, so it may not precisely reflect the atrial effects of RFA, such as local conduction in the atria and AVN. Further study is warranted to investigate underlying mechanisms by using a mapping system to perform ex vivo mapping with direct ablation of the $GP_{IVC\text{-}LA}$ epicardially.

Conclusions

In canines, RFA at the bottom of Koch's triangle impaired the $GP_{IVC\text{-}ICA}$ and attenuated local autonomic innervation in the AVN and atrial tissue, which might contribute to VS-induced discontinuous AVN conduction and atrial ERP shortening. Moreover, in SVT patients, RFA of the slow pathway within Koch's triangle prolonged local atrial ERPs and decreased AF inducibility. These findings suggested that in certain types of AF, such as vagal AF, the effect of slow-pathway ablation on

AF might be related to the denervation of local autonomic nerves.

Sources of Funding

This work was supported by external grants to Yin from Liaoning Province (201201009, L2011154, 2015020259, 201501853) and from the Chinese Ministry of Health (w201003). It was also supported by internal grants from Dalian Medical University.

Disclosures

None.

References

1. Kocovic DZ, Harada T, Shea JB, Soroff D, Friedman PL. Alterations of heart rate and of heart rate variability after radiofrequency catheter ablation of supraventricular tachycardia. Delineation of parasympathetic pathways in the human heart. *Circulation*. 1993;88:1671–1681.
2. Havranek S, Souckova L, Simek J, Wichterle D. Slow pathway ablation for typical atrioventricular nodal re-entrant tachycardia significantly alters the autonomic modulation of atrioventricular conduction. *Clin Auton Res*. 2013;23:289–295.
3. Razavi M, Cheng J, Rasekh A, Yang D, Delapasse S, Ai T, Meade T, Donsky A, Goodman MJ, Massumi A. Slow pathway ablation decreases vulnerability to pacing-induced atrial fibrillation: possible role of vagal denervation. *Pacing Clin Electrophysiol*. 2006;29:1234–1239.
4. Markowitz SM, Christini DJ, Stein KM, Mittal S, Iwai S, Slotwiner DJ, Lerman BB. Time course and predictors of autonomic dysfunction after ablation of the slow atrioventricular nodal pathway. *Pacing Clin Electrophysiol*. 2004;27:1638–1643.
5. Kowallik P, Escher S, Peters W, Braun C, Meesmann M. Preserved autonomic modulation of the sinus and atrioventricular nodes following posteroseptal ablation for treatment of atrioventricular nodal reentrant tachycardia. *J Cardiovasc Electrophysiol*. 1998;9:567–573.
6. Kautzner J, Hartikainen J, Heald S, Malik M, Ward D, Rowland E. Is vagal innervation to the atrioventricular node impaired after radiofrequency ablation of the slow atrioventricular nodal pathway? *Pacing Clin Electrophysiol*. 1996;19:1993–1997.
7. Wilhelmy R, Pitschner H, Neuzner J, Dursch M, Konig S. Patients with AV nodal reentrant tachycardias show a reduced vagal impact on heart rate compared to healthy subjects with further decrease of vagal tone after radiofrequency catheter modification. *Clin Sci (Lond)*. 1996;91(suppl):125.
8. Hou Y, Scherlag BJ, Lin J, Zhang Y, Lu Z, Truong K, Patterson E, Lazzara R, Jackman WM, Po SS. Ganglionated plexi modulate extrinsic cardiac autonomic nerve input: effects on sinus rate, atrioventricular conduction, refractoriness, and inducibility of atrial fibrillation. *J Am Coll Cardiol*. 2007;50:61–68.
9. Quan KJ, Lee JH, Van Hare GF, Biblo LA, Mackall JA, Carlson MD. Identification and characterization of atrioventricular parasympathetic innervation in humans. *J Cardiovasc Electrophysiol*. 2002;13:735–739.
10. Ardell JL, Randall WC. Selective vagal innervation of sinoatrial and atrioventricular nodes in canine heart. *Am J Physiol*. 1986;251:H764–H773.
11. Lin J, Scherlag BJ, Niu G, Lu Z, Patterson E, Liu S, Lazzara R, Jackman WM, Po SS. Autonomic elements within the ligament of Marshall and inferior left ganglionated plexus mediate functions of the atrial neural network. *J Cardiovasc Electrophysiol*. 2009;20:318–324.
12. Hayashi H, Usui M, Tani M, Nagasawa H, Fujiki A, Inoue H. Radiofrequency ablation at the coronary sinus ostium interrupts the vagal efferent input to the atrioventricular node in the canine heart. *Jpn Circ J*. 2001;65:667–672.
13. Soejima K, Akaishi M, Mitamura H, Ogawa S, Sakurada H, Okazaki H, Motomiya T, Hiraoka M. Increase in heart rate after radiofrequency catheter ablation is mediated by parasympathetic nervous withdrawal and related to site of ablation. *J Electrocardiol*. 1997;30:239–246.
14. Sauer WH, Alonso C, Zado E, Cooper JM, Lin D, Dixit S, Russo A, Verdino R, Ji S, Gerstenfeld EP, Callans DJ, Marchlinski FE. Atrioventricular nodal reentrant tachycardia in patients referred for atrial fibrillation ablation: response to ablation that incorporates slow-pathway modification. *Circulation*. 2006;114:191–195.
15. Wyndham CR, Amat-y-Leon F, Wu D, Denes P, Dhingra R, Simpson R, Rosen KM. Effects of cycle length on atrial vulnerability. *Circulation*. 1977;55:260–267.
16. Razavi M, Zhang S, Yang D, Sanders RA, Kar B, Delapasse S, Ai T, Moreira W, Olivier B, Khoury DS, Cheng J. Effects of pulmonary vein ablation on regional atrial vagal innervation and vulnerability to atrial fibrillation in dogs. *J Cardiovasc Electrophysiol*. 2005;16:879–884.
17. Morillo CA, Klein GJ, Jones DL, Guiraudon CM. Chronic rapid atrial pacing. Structural, functional, and electrophysiological characteristics of a new model of sustained atrial fibrillation. *Circulation*. 1995;91:1588–1595.
18. Po SS, Nakagawa H, Jackman WM. Localization of left atrial ganglionated plexi in patients with atrial fibrillation. *J Cardiovasc Electrophysiol*. 2009;20:1186–1189.
19. Moe GK, Preston JB, Burlington H. Physiologic evidence for a dual A-V transmission system. *Circ Res*. 1956;4:357–375.
20. Denes P, Wu D, Dhingra RC, Chuquimia R, Rosen KM. Demonstration of dual A-V nodal pathways in patients with paroxysmal supraventricular tachycardia. *Circulation*. 1973;48:549–555.
21. Belhassen B, Fish R, Glikson M, Glick A, Eldar M, Laniado S, Viskin S. Noninvasive diagnosis of dual AV node physiology in patients with AV nodal reentrant tachycardia by administration of adenosine-5′-triphosphate during sinus rhythm. *Circulation*. 1998;98:47–53.
22. Wit AL, Weiss MB, Berkowitz WD, Rosen KM, Steiner C, Damato AN. Patterns of atrioventricular conduction in the human heart. *Circ Res*. 1970;27:345–359.
23. Chiou CW, Chen SA, Kung MH, Chang MS, Prystowsky EN. Effects of continuous enhanced vagal tone on dual atrioventricular node and accessory pathways. *Circulation*. 2003;107:2583–2588.
24. Mazgalev T, Dreifus LS, Michelson EL, Pelleg A. Effect of postganglionic vagal stimulation on the organization of atrioventricular nodal conduction in isolated rabbit heart tissue. *Circulation*. 1986;74:869–880.
25. Mazgalev T, Dreifus LS, Michelson EL, Pelleg A. Vagally induced hyperpolarization in atrioventricular node. *Am J Physiol*. 1986;251:H631–H643.
26. Mazgalev T, Dreifus LS, Michelson EL, Pelleg A, Price R. Phasic effects of postganglionic vagal stimulation on atrioventricular nodal conduction. *Am J Physiol*. 1986;251:H619–H630.
27. Prystowsky EN. Atrioventricular node reentry: physiology and radiofrequency ablation. *Pacing Clin Electrophysiol*. 1997;20:552–571.
28. Tai CT, Chen SA, Chiang CE, Lee SH, Wen ZC, Chiou CW, Ueng KC, Chen YJ, Yu WC, Huang JL, Chang MS. Complex electrophysiological characteristics in atrioventricular nodal reentrant tachycardia with continuous atrioventricular node function curves. *Circulation*. 1997;95:2541–2547.
29. Chiou CW, Eble JN, Zipes DP. Efferent vagal innervation of the canine atria and sinus and atrioventricular nodes. The third fat pad. *Circulation*. 1997;95:2573–2584.
30. Zhou J, Scherlag BJ, Edwards J, Jackman WM, Lazzara R, Po SS. Gradients of atrial refractoriness and inducibility of atrial fibrillation due to stimulation of ganglionated plexi. *J Cardiovasc Electrophysiol*. 2007;18:83–90.